Journal of the American Heart Association

ORIGINAL RESEARCH

ELM2-SANT Domain-Containing Scaffolding Protein 1 Regulates Differentiation and Maturation of Cardiomyocytes Derived From Human-Induced Pluripotent Stem Cells

Yu-An Lu, PhD*; Jiacheng Sun, MD, PhD*; Lu Wang, PhD; Meimei Wang, MSc; Yalin Wu, MD; Anteneh Getachew, PhD; Rachel C. Matthews, BS; Hui Li, BS; William Gao Peng; Jianyi Zhang, MD, PhD; Rui Lu, PhD; Yang Zhou, PhD

BACKGROUND: ELMSAN1 (ELM2-SANT domain-containing scaffolding protein 1) is a newly identified scaffolding protein of the MiDAC (mitotic deacetylase complex), playing a pivotal role in early embryonic development. Studies on *Elmsan1* knockout mice showed that its absence results in embryo lethality and heart malformation. However, the precise function of ELMSAN1 in heart development and formation remains elusive. To study its potential role in cardiac lineage, we employed human-induced pluripotent stem cells (hiPSCs) to model early cardiogenesis and investigated the function of ELMSAN1.

METHODS AND RESULTS: We generated *ELMSAN1*-deficient hiPSCs through knockdown and knockout techniques. During cardiac differentiation, *ELMSAN1* depletion inhibited pluripotency deactivation, decreased the expression of cardiac-specific markers, and reduced differentiation efficiency. The impaired expression of genes associated with contractile sarcomere structure, calcium handling, and ion channels was also noted in *ELMSAN1*-deficient cardiomyocytes derived from hiPSCs. Additionally, through a series of structural and functional assessments, we found that *ELMSAN1*-null hiPSC cardiomyocytes are immature, exhibiting incomplete sarcomere Z-line structure, decreased calcium handling, and impaired electrophysiological properties. Of note, we found that the cardiac-specific role of ELMSAN1 is likely associated with histone H3K27 acetylation level. The transcriptome analysis provided additional insights, indicating maturation reduction with the energy metabolism switch and restored cell proliferation in *ELMSAN1* knockout cardiomyocytes.

CONCLUSIONS: In this study, we address the significance of the direct involvement of ELMSAN1 in the differentiation and maturation of hiPSC cardiomyocytes. We first report the impact of ELMSAN1 on multiple aspects of hiPSC cardiomyocyte generation, including cardiac differentiation, sarcomere formation, calcium handling, electrophysiological maturation, and proliferation.

Key Words: acetylation ■ cardiomyocyte ■ ELMSAN1 ■ hiPSC ■ maturation ■ MiDAC

The heart is the first functional organ in vertebrate embryos.[1] Cardiogenesis is the process of heart formation during embryonic development. It is a complex and tightly regulated process that involves a series of molecular and cellular events, including cell migration, proliferation, differentiation, specification, and maturation.[2] The precise cardiogenesis depends on the timely activation of developmental molecular

Correspondence to: Yang Zhou, PhD, Department of Biomedical Engineering, University of Alabama at Birmingham, 1825 University Blvd, Birmingham, AL 35233. Email: yangzhou@uab.edu

*Y.-A. Lu and J. Sun contributed equally.

This article was sent to Sakima A. Smith, MD, MPH, Associate Editor, for review by expert referees, editorial decision, and final disposition.

Supplemental Material is available at https://www.ahajournals.org/doi/suppl/10.1161/JAHA.124.034816

For Sources of Funding and Disclosures, see page 17.

JAHA is available at: www.ahajournals.org/journal/jaha

RESEARCH PERSPECTIVE

What Is New?

- Loss of the epigenetic gene *ELMSAN1* (ELM2-SANT domain-containing scaffolding protein 1) disrupts the differentiation and maturation of human-induced pluripotent stem cell-derived cardiomyocytes.
- The Class I histone MiDAC (mitotic deacetylase complex), which has been underexplored, plays crucial roles in cardiomyocyte differentiation by regulating sarcomere structure formation, calcium handling, and electrophysiological properties.

What Question Should Be Addressed Next?

- Investigating whether and how the MiDAC complex contributes to embryonic heart development or cardiac disease development in vivo.
- Elucidating the mechanistic role of the MiDAC complex on regulating histone or nonhistone acetylation.

Nonstandard Abbreviations and Acronyms

CoREST	corepressor of repressor element-1 silencing transcription factor complex
HDACs	histone deacetylases
MiDAC	mitotic deacetylase complex
NuRD	nucleosome remodeling and deacetylating
Sin3	switch-independent protein 3

cascades that are spatially and temporally controlled by transcription factors and epigenetic modulators.[3,4] However, this sophisticated regulatory system can be vulnerable to perturbations, leading to congenital heart disease and structural defects.[5] Increasing evidence indicates that epigenetic regulation plays a critical role in cardiac development and disease,[6,7] particularly in the regulation of cardiac lineage commitment through DNA methylation and histone modification.[8] Nevertheless, the detailed mechanisms by which epigenetic factors coordinate with transcriptional factors to orchestrate cardiogenesis gene programs are not yet fully understood. Further study may lead to a better understanding of the causes of congenital heart disease and the development of new therapies to treat these conditions.

Histone acetylation, one of the major posttranslational modifications of histones, serves as a critical modulator of chromatin remodeling and gene transcription.[9] Acetylation of the lysine residues in the histone tails via histone acetyltransferases increases chromatin accessibility by neutralizing positive charge to loosen chromatin structures associated with gene activation.[10] On the other hand, histone deacetylases (HDACs) remove acetyl groups from histone tails, leading to chromatin condensation and transcriptional repression.[11] HDAC1 and HDAC2 (HDAC1/2) are closely related class I HDACs that mainly form the catalytic core of multiple corepressor complexes, including nucleosome remodeling and deacetylating (NuRD), Sin3 (switch-independent protein 3), CoREST (co-repressor of repressor element-1 silencing transcription factor complex), and MiDAC (mitotic deacetylase complex).[12-14] The formation of these complexes is essential for HDAC1/2 activity and recruitment toward the specific substrates. The potential roles of HDAC1/2 in cardiac lineage commitment have been demonstrated in different systems.[15] The germline depletion of *HDAC1* alleles results in embryonic lethality before embryonic day E10.5 due to severe proliferation defects,[16] which have also been observed in *HDAC1*-null embryonic stem cells.[17] Cardiac-specific deletion of *HDAC1/2* together results in neonatal lethality, accompanied by arrhythmias and dilated cardiomyopathy.[18] In addition, the loss of *HDAC1* impairs differentiation and maturation of cardiomyocytes derived from pluripotent stem cells.[19]

Unlike NuRD, Sin3, and CoREST complexes, whose molecular functions have been largely investigated,[20] MiDAC is a newly identified tetrameric complex containing HDAC1/2, ELMSAN1 (ELM2-SANT domain-containing scaffolding protein 1; also known as MIDEAS), and scaffolding protein DNTTIP1 (deoxynucleotidyltransferase terminal interacting protein 1).[21,22] The MiDAC complex is associated with mitotic processes.[23] The knockdown of MiDAC by siRNA interference in mouse embryonic fibroblasts leads to mitotic chromatin misalignment.[23] Recently, the role of MiDAC has been revealed in neural differentiation and embryonic development.[24] During neurogenesis, MiDAC controls genes associated with neurite outgrowth by regulating H4K20ac and H3K27ac levels.[25] Additionally, homozygous mice embryos lacking ELMSAN1 die after embryonic day E16.5 with severe anemia and heart malformation,[23] suggesting an underestimated role of ELMSAN1 in developing hearts.

To gain insight into the developmental role of ELMSAN1 in cardiac lineage commitment, we generated *ELMSAN1*-deficient human-induced pluripotent stem cells (hiPSCs) using shRNA for knockdown and the CRISPR/Cas9 system for knockout. Subsequently, we conducted a comprehensive series of assessments for the differentiation and maturation parameters of cardiomyocytes derived from hiPSCs (hiPSC-CMs). We then documented a required role of ELMSAN1 for cardiac differentiation and functional maturation,

followed by our findings that ELMSAN1 is enriched in hiPSC-CMs, and its absence leads to reduced H3K27ac and a transcriptional program that impairs cardiomyocyte maturation. Therefore, our study underscores the undocumented role for ELMSAN1 and MiDAC in regulating cardiomyocyte differentiation and promoting functional maturation.

METHODS

The data, analytical methods, and study materials are available from the corresponding author upon reasonable request. All genomic data sets have been deposited in the Gene Expression Omnibus under accession number GSE262838 and are publicly accessible. No animals were involved in this study. The Institutional Review Board of the University of Alabama at Birmingham has reviewed our use of human cells, confirming that it does not constitute human subject research.

Preparation of *ELMSAN1* Knockdown and Knockout Viral Particles

To generate the *ELMSAN1* knockdown stable line, pLKO.1-blast (Addgene#26655) and pLKO.1-shELMSAN1 (shELMSAN1: 5′-CCTCTACTTCAATGCCATCAT—3′) plasmids were used as indicated. Lentiviral vector pLentiCRISPRv2Blast (Addgene #98293) was used for CRISPR knockout *ELMSAN1* (sgELMSAN1: 5′—GGCCTCAACTACCAAGTGTG—3′). For lentivirus packaging, pMD2G and psPAX2 were purchased from Addgene. Corresponding viral and package plasmids were transfected with NanoFect (ALSTEM) into HEK293T cells. Lentivirus supernatants were collected 48 and 72 hours after transfection and passed through a 0.22 μm filter. The virus particles were further precipitated with 8% PEG6000 overnight and collected via centrifugation at 4000 rpm for 30 minutes at 4 °C. The aliquots were used for hiPSC infection.

hiPSC Culture and Generation of *ELMSAN1* Knockdown and Knockout Stable Lines

The hiPSCs were cultured in the Geltrex-coated (Gibco) 6-well plate with mTeSR Plus medium (STEMCell Technologies, Canada). For infection, in 1 well of a 6-well plate, 10 μL of concentrated lentiviruses was transduced into approximately 50% confluent iPSCs for 2 days in 1 mL antibiotic-free mTeSR medium with 8 μg/mL polybrene. Two days after virus transduction, hiPSCs were cultured in fresh mTeSR medium and treated with blasticidin (6 μg/mL) for another 48 hours. The medium containing blasticidin was replaced every 2 days until colonies attained sufficient size and cell density for differentiation. A single colony of ELMSAN1-knockout (KO) line was generated by serial dilution in a 96-well plate and validated by Sanger sequencing analysis for genomic sequences.

Cardiomyocyte Differentiation From hiPSCs

Human iPSCs were seeded in Geltrex coated 6-well plates at a density of 2.5×10^5 cells/cm^2 on Day –1. Differentiation was initiated on differentiation Day 0 by replacing mTeSR medium with 2 mL RPMI 1640 culture medium supplemented with B27 without insulin (RPMI/B27 minus) and treated with an additional 10 μmol/L CHIR99021 (STEMCell Technologies) at a 90% to 100% confluency. On Day 1, the medium was replaced with 2 mL RPMI/B27 minus with 3 μmol/L CHIR99021, and cells were incubated for 2 days. On Day 3, the medium was replaced with RPMI/B27 minus supplemented with 10 μmol/L IWP-2 (STEMCell Technologies). On Day 5, the culture medium was changed to freshly prepared RPMI/B27 minus for 48 hours. On Day 7, medium was changed to RPMI 1640 culture medium supplemented with B27 with insulin (RPMI/B27 plus). The differentiated cardiomyocytes (after Day 7) were maintained in RPMI/B27 plus with fresh medium changes every 2 days. All differentiated cardiomyocytes showed spontaneous beating on Day 7. A schematic representation of the protocol was shown in Figure S1B.

Cells were maintained in the same well from Day –1 to Day 9 until harvested for assays such as real-time quantitative polymerase chain reaction (qPCR), chromatin immunoprecipitation-qPCR, Western blot, flow cytometry, transmission electron microscopy, and RNA sequencing. For assays that required replating cells, such as microelectrode array (MEA assay), calcium transient evaluation, and immunofluorescent staining, Day 7 hiPSC-CMs were dissociated with the STEMdiff cardiomyocyte dissociation kit (STEMCell Technologies), replated to the microelectrode plate, cover glass, or chamber slides, respectively, and allowed to recover for 2 days before the experiments. For assays that required purified cardiomyocytes, cardiomyocytes were purified using metabolic starvation. Briefly, culture medium was changed on Day 9 to the purification medium (RPMI 1640, no glucose supplemented with B27 plus and 4 mmol/L sodium DL-lactate solution). Cardiomyocytes were maintained in the purification medium for 6 consecutive days with medium changes every 3 days. On Day 15, purified cardiomyocytes were replated to chamber slides, maintained in RPMI/B27 plus, and allowed to recover for 2 days before being subjected to immunofluorescent staining.

Flow Cytometry

Cells were dissociated using trypsin, then pelleted by centrifugation at 200*g* for 5 minutes. The manufacturer's protocol used a fixation/permeabilization solution (BD Biosciences, San Diego, CA). The fixed cells were washed 2 times with 10% BD Perm/Wash buffer (BD Biosciences). Samples were incubated with the primary antibody of cTnT (cardiac troponin T), which was 1:400 diluted in BD Perm/Wash buffer at 4 °C for 45 minutes in the dark.

Gene Expression By Real-Time Quantitative PCR

Total RNA was extracted using TRIzol reagent, and cDNA was synthesized using Protoscript Reverse Transcriptase (New England Biolabs). The amplified samples were measured by SYBR Green mix and incorporated with the QuantStudio Real-Time PCR system. The primers used in the present study are listed in Table S1. All the gene expressions were normalized to the housekeeping gene GADPH.

RNA-Seq and Data Analysis

RNA-seq libraries were prepared following the manufacturer's instructions using the NEBNext Ultra RNA Library Prep Kit for Illumina from New England Biolabs. The quality and concentration of these libraries were assessed using the Bioanalyzer High Sensitivity DNA Chip by Agilent. Subsequently, multiplexed RNA-Seq libraries were subjected to paired-end sequencing for 150 base pairs on the Illumina HiSeq 4000 platform. For alignment to the human genome (hg19), the paired-end reads underwent mapping using STAR (v2.5.1b) with default parameters. Read counts were extracted and employed for differential gene expression analysis using DESeq2 (v3.11). K-means clustering and heatmaps were produced using ComplexHeatmap (v2.18). Gene ontology analysis was performed using the enrichR database. To evaluate gene expression signatures, we conducted gene set variation analysis, incorporating gene sets sourced from the Molecular Signatures Database as well as customized gene sets from prior studies.[26,27]

Chromatin Immunoprecipitation-qPCR

For each chromatin immunoprecipitation reaction, we collected 100 000 cells at Day 9 of differentiation from both wild-type (WT) or ELMSAN1-KO hiPSC-CMs. These samples were then processed using the MAGnify Chromatin Immunoprecipitation System kit (Invitrogen Life Technologies) following the manufacturer's instructions. H3K27ac antibody (Abcam #ab4729) and IgG (included in the MAGnify Kit) were used for the immunoprecipitation. qPCR was performed using 2x SYBR Green PCR master mix (Bimake, B21202) on the CFX Opus 384 Real-674 Time PCR system (BIO-RAD). For the data analysis, the CT (cycle threshold) values were normalized to input controls. Statistical significance between groups was determined using 2-way ANOVA. The primers employed for qPCR are detailed in Table S2.

Calcium Transient Evaluation

The calcium transients were measured using the method previously described.[28] Briefly, D7 iPSC-CMs were dissociated, replated on Geltrex-coated cover glasses (25×25 mm), and allowed to recover for 2 days. On Day 9, the iPSC-CMs were incubated with 0.5 µmol/L Fura-2 AM (Invitrogen, USA) for 10 minutes in Tyrode's solution, and washed for another 10 minutes with normal Tyrode's solution at room temperature before calcium measurements. The ratio of fluorescence emitted at 340 and 380 nm was recorded during 1 Hz field stimulation in Tyrode's solution using a calcium recording system. The resulting data were analyzed with IonWizard software (IonOptix, USA).

Immunofluorescence and Confocal Microscopy

iPSC-CMs were fixed with 4% paraformaldehyde in PBS for 10 minutes at room temperature. After being rinsed twice in PBS, the samples were permeabilized with chilled 90% acetone in PBS for 3 minutes, blocked with 5% donkey serum for 30 minutes, conjugated with primary antibodies (Table S3) at 4 °C overnight, and with fluorescently conjugated secondary antibodies for 1 hour at room temperature. Images were obtained with a confocal microscope (Olympus, Japan).

Western Blot Analysis

The cells were lysed in the whole-cell lysis buffer and separated by SDS-PAGE. The primary and secondary antibodies are summarized in Table S4.

Microelectrode Array-Based Analysis of Cell Behavior

MEAs are also known as multielectrode arrays, which are composed of many dot-like electrodes embedded in the culture surface of the well. Electrically active cardiomyocytes were cultured on top of the electrodes. CytoView MEA 24 well plates (Axion Biosystems, Atlanta, GA) were precoated with Geltrex and incubated at 37 °C for 1 hour. After dissociating the cardiomyocytes from 6 cell plates, 100 000 cells per well were seeded on the electrode of the CytoView MEA

24 well plate, and data were acquired after 48 hours. Field potential and contractility measurements were recorded with Axion BioSystems' Integrated Studio software version 2.4 (Axion Biosystems) and action potential durations were monitored with the L1 element amplification protocol assay and characterized with the Cardiac Analysis Tool software (Axion Biosystems).

Transmission Electron Microscopy

Approximately 1.2×10^7 control or ELMSAN1-KD hiPSC-CMs were washed twice with PBS and fixed in the 2.5% glutaraldehyde solution for at least 30 minutes at 4 °C. The cells were then scraped into a 1.5 mL Eppendorf tube and centrifuged at 500*g* for 5 minutes. The visualizable cell pellets were delivered to the UAB High-Resolution Imaging Facility. A Tecnai Spirit T12 Transmission Electron Microscope was used to examine the samples. For each group, at least 3 images were collected, and sarcomere lengths and widths were determined for all sarcomeres in an image using ImageJ's line-measure tool. Sarcomere lengths were calculated as the distance between Z-lines, and widths were calculated as the distance between the ends of a continuous Z-line.

Statistical Analysis

Statistics were calculated in GraphPad Prism 9 and R, version 4.0.4. All data passed the normality check using Shapiro–Wilk and Kolmogorov–Smirnov tests. Two-group testing was performed using paired or unpaired 2-tailed Student *t* test as indicated. Then 1-way or 2-way ANOVA was used for multigroup significance testing followed by adjustment where indicated for multiple comparisons. In all tests, $P<0.05$ was considered significant.

RESULTS

Depletion of *ELMSAN1* Impairs Cardiomyocyte Differentiation of hiPSCs

To determine the role of ELMSAN1 in cardiogenesis, we first generated a stable *ELMSAN1* knockdown (ELMSAN1-KD) hiPSC line, which exhibited typical hiPSC morphology (Figure S1A) and ~50% knockdown of ELMSAN1 protein level (Figure 1A). We also confirmed the knockdown of *ELMSAN1* mRNA expression by approximately 50% compared with control along the process of cardiomyocyte differentiation following the GiWi protocol[29] (Figure 1B and Figure S1B). Flow cytometry analysis at differentiation Day 9 showed a decreased percentage of cTnT (cardiac troponin T) positive cells and a reduced forward scatter area measurement in ELMSAN1-KD hiPSCs compared with the control group (Figure 1C), suggesting that *ELMSAN1* depletion results in less efficient differentiation of cardiomyocytes with smaller morphology. Specifically, time-course gene expression analysis showed that ELMSAN1 depletion resulted in a relatively high expression of pluripotency markers, including octamer-binding transcription factor 4 (*OCT4*) and NANOG homeobox (*NANOG*), during the early mesoderm differentiation (Figure 1D). In ELMSAN1-KD cells, we observed a delayed expression of mesoderm marker mesoderm posterior bHLH transcription factor 1 (*MESP1*), which might be associated with incomplete loss of pluripotency genes. Interestingly, cardiac progenitor markers insulin gene enhancer protein (*ISL1*) and NK2 homeobox 5 (*NKX2-5*) were significantly upregulated in ELMSAN-KD cells after 9 days of cardiac differentiation, whereas cardiomyocyte-specific troponin T2, cardiac type (*TNNT2*), and alpha-actinin-2 (*ACTN2*) were decreased (Figure 1D), suggesting immature cardiac differentiation in ELMSAN1-KD cells. Our results demonstrate that ELMSAN1 is required for efficient differentiation of iPSC-CMs.

ELMSAN1 Depletion Reduces the Expression of Cardiomyocyte Maturation-Associated Genes

At Day 7 of iPSC-CM differentiation, we observed differential rhythmical contracting in the ELMSAN1-KD group (Videos S1 and S2), suggesting the involvement of ELMSAN1 in cardiomyocyte functional maturation. To investigate the molecular characteristics underlying this phenotype, we examined the expression of a panel of genes associated with sarcomere structure, calcium handling, and ion channels in ELMSAN1-KD and control iPSC-CMs. Our real-time-qPCR results demonstrated a significant reduction in the expression of sarcomere structural genes, including cardiac troponin-I (*TNNI3*), actin alpha cardiac muscle 1 (*ACTC1*), and α-myosin heavy chain (*MYH6*) (Figure 2A). Calcium handling and contractility, as the critical features of the cardiomyocyte maturity,[30] were evaluated by the expression of ryanodine receptor 2 (*RYR2*), ATPase sarcoplasmic/endoplasmic reticulum Ca^{2+} transporting 2 (*ATP2A2*), Cav1.2 L-type voltage-gated calcium channel (*CACNA1C*), and phospholamban (*PLN*). At Day 9 of differentiation, all the calcium-handling markers mentioned were remarkably decreased in ELMSAN1-KD cells (Figure 2B). An additional set of ion channel genes, such as solute carrier family 8 member A1 (*SLC8A1*), potassium inwardly rectifying channel subfamily J member 2 (*KCNJ2*), gap junction protein alpha 1 (*GJA1*), and cadherin 2 (*CDH2*), was downregulated

following ELMSAN1 knockdown. Moreover, immunofluorescence staining analysis demonstrated the reduced protein expression of SERCA, N-Cadherin, and Kir2.1 in ELMSAN1-KD group at the single cell level (Figure 2D). These findings collectively suggest that ELMSAN1 plays a crucial role in the induction

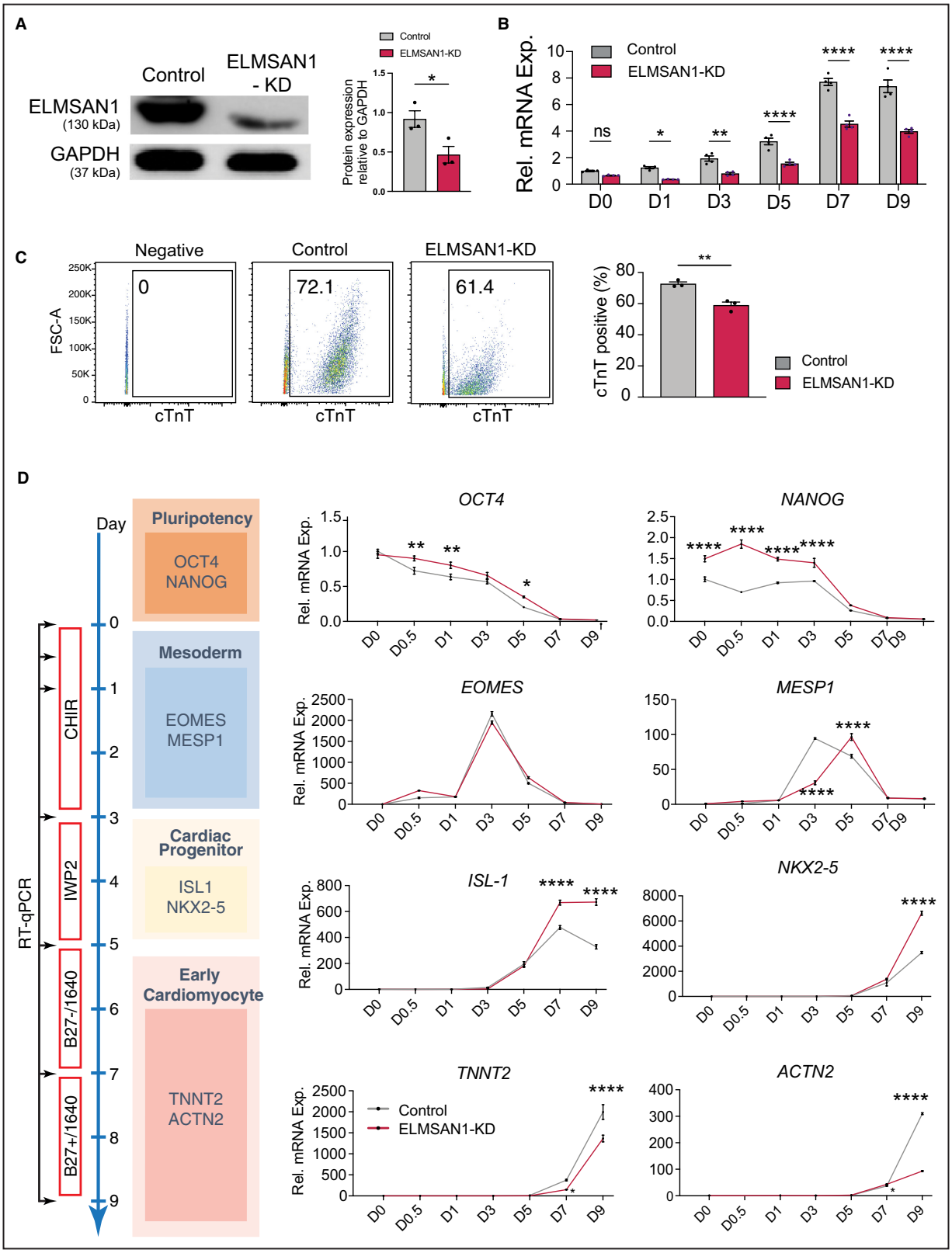

Figure 1. Knockdown of *ELMSAN1* represses cardiac differentiation and delays the loss of pluripotency.
A, Western blot results of ELMSAN1 reduction in control and *ELMSAN1* knockdown hiPSCs. GAPDH is used as an internal control for ELMSAN1 expression quantification (n=3). **B**, *ELMSAN1* knockdown efficiency was evaluated by RT-qPCR on different time points as indicated during cardiac differentiation process. **C**, Flow cytometry analysis showed reduced percentage of cTnT positive cells in ELMSAN1-KD hiPSC-CMs. **D**, Time course expression changes of pluripotency markers *OCT4* and *NANOG*; mesoderm markers *EOMES* and *MESP1*; cardiac progenitor markers *ISL-1* and NKX2-5; cardiomyocyte makers *TNNT2* and *ACTN2* in the control group and ELMSAN1-KD group were analyzed by RT-qPCR and normalized to *GAPDH* (n=3). Data are presented as mean±SEM (**B** and **D**, 2-way ANOVA; **C**, Student *t* test). n.s. ($P>0.05$), *$P<0.05$, **$P<0.01$, ****$P<0.0001$. cTnT indicates cardiac troponin T; ELMSAN1, ELM2-SANT domain-containing scaffolding protein 1; ELMSAN1-KD, ELM2-SANT domain-containing scaffolding protein 1 knockdown; FSC-A, forward scatter area; hiPSC-CM, employed human-induced pluripotent stem cell cardiomyocyte; and RT-qPCR, reverse transcription quantitative polymerase chain reaction.

of maturation-related gene programs, including sarcomere structure, calcium handling, and ion channels.

ELMSAN1-KD hiPSC-CMs Exhibit Immature Sarcomeres and Impaired Calcium Handling

Next, we performed a series of structural and functional assessments on ELMSAN1-KD hiPSC-CMs to determine the effects of ELMSAN1 on cardiomyocyte maturation. The immunostaining of cTnI (cardiac troponin I) and α-Actinin (cardiac alpha actinin), which indicates the sarcomere thin filament and Z-line, respectively, showed a decrease in myofibril density and a less organized sarcomere alignment in ELMSAN1-KD hiPSC-CMs compared with control cells (Figure 3A). Quantification of the distance between Z-lines further suggested that loss of *ELMSAN1* in hiPSC-CMs led to a significant decrease in sarcomere length (1.3 μm in ELMSAN1-KD versus 1.5 μm in control group, $P<0.001$). Transmission electron microscopy results also revealed the differences in myofibril alignment and ultrastructural morphology (Figure 3B): the control hiPSC-CMs displayed typical Z-lines and nascent sarcomere structures, whereas highly underdeveloped contractile units were identified with incomplete Z-lines and disordered sarcomere filaments in the ELMSAN1-depleted cardiomyocytes. The findings demonstrate that ELMSAN1 is required for the structural maturation of hiPSC-CMs.

Moreover, to determine whether the reduced gene expression of calcium-related markers upon *ELMSAN1* loss (Figure 2B) is accompanied by impaired calcium handling, we examined the calcium transient parameters in both control and ELMSAN1-KD hiPSC-CMs. The fura-2 calcium indicator was used to visualize calcium transients in purified ELMSAN1-KD and control hiPSC-CMs at differentiation Day 12 (Figure 3C through 3E). We observed a significant decrease in the amplitude of calcium transients (Figure 3D) and an increased trend of time to peak 10% value in the ELMSAN1-KD group (Figure 3E). The weakened calcium transient observed in *ELMSAN1*-depleted cardiomyocytes further demonstrated the critical role of ELMSAN1 in regulating hiPSC-CM maturation.

ELMSAN1 Disruption Interferes With Electrophysiological Behaviors of hiPSC-CMs

Electrical impulses and oscillations of cytoplasmic Ca^{2+} concentration tightly control the force, speed, and rhythm of cardiomyocyte contraction and relaxation. To study the effects of *ELMSAN1* disruption on the electrophysiological behaviors of hiPSC-CMs, we conducted MEA assays.[31,32] The electrical and beating activity of hiPSC-CMs were recorded using noninvasive techniques and measured by electrodes in the MEA plate without compromising the membrane integrity (Figure S2A). The results showed that ELMSAN1-KD hiPSC-CMs exhibited an increased spontaneous beat rate (Figure 4A) with a shorter beat period (1.26 seconds versus 1.50 seconds, $P<0.001$) and a reduced beat amplitude compared with the control (Figure 4B through 4C). Meanwhile, slower cardiac beat propagation (Figure 4D and Figure S2B) and reduced conduction velocity (Figure 4E) were observed with *ELMSAN1* depletion. The longer excitation-contraction delay was also measured in ELMSAN1-KD cells (Figure 4F). All these data suggest that *ELMSAN1* deficiency disrupts the excitation-contraction coupling of hiPSC-CMs.
Two important parameters of cardiac electrophysiology, field potential duration and spike amplitude, were also analyzed. The ELMSAN1-KD group exhibited a significantly shorter field potential duration compared with the control group (311.89±23.43 milliseconds versus 520.05±33.63 ms, respectively, $P<0.001$) as well as a lower spike amplitude (0.48±0.083 mV versus 1.83±0.015 mV, $P<0.001$; Figure 4G), supporting an impaired electrophysiological phenotype in the *ELMSAN1* depletion group. Taken together, ELMSAN1 is required for hiPSC-CM maturation in terms of gene expression, sarcomere formation, calcium handling, and electrophysiology.

ELMSAN1 Knockout Results in Similar Phenotypes in iPSC-CM Differentiation and Maturation

To exclude the potential off-target effects of the RNAi-mediated knockdown in the polyclonal iPSC lines, we

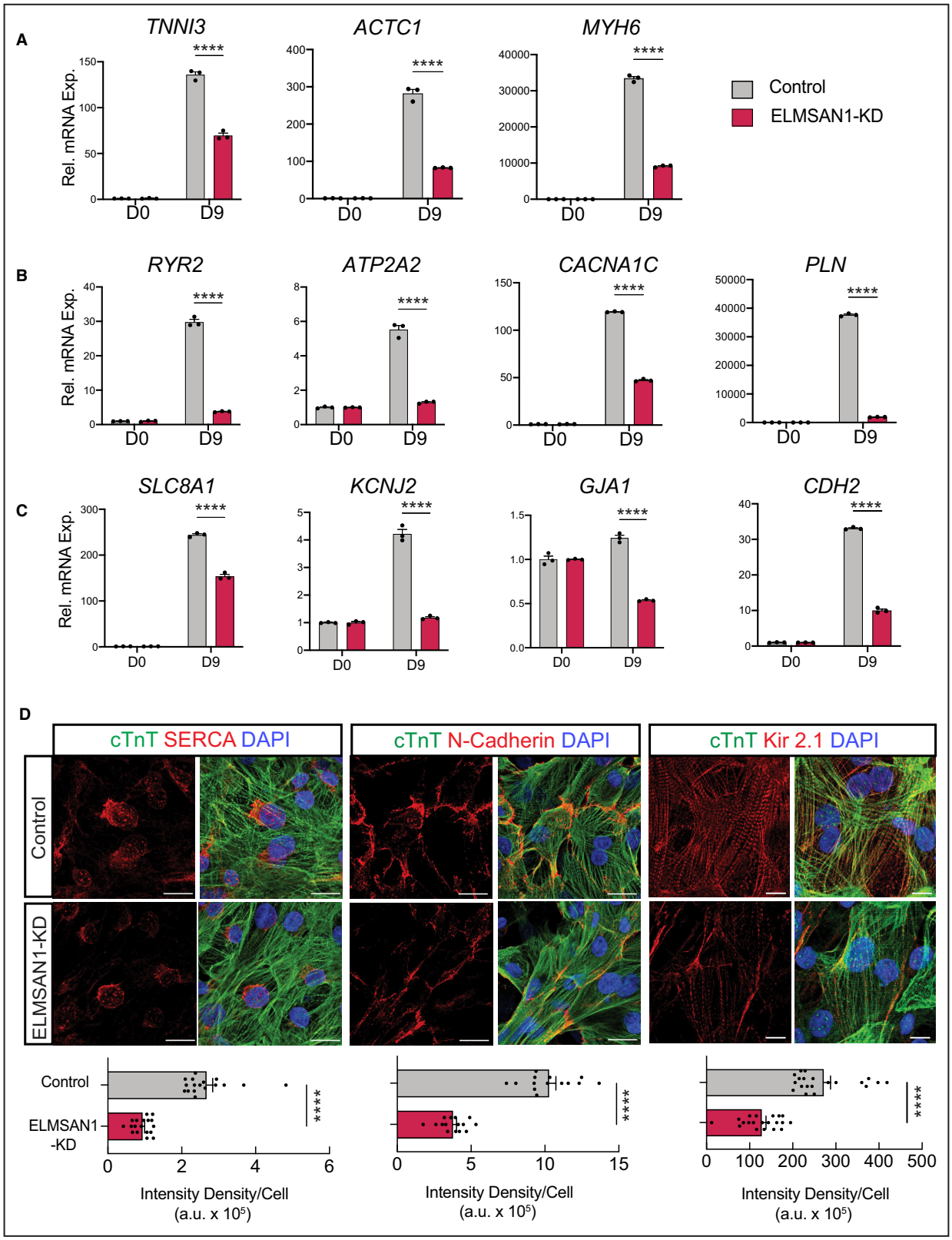

generated monoclonal iPSC lines by CRISPR/Cas9-based *ELMSAN1* knockout and evaluated cardiac differentiation and maturation. ELMSAN1 transcript was evaluated by real-time-qPCR for the primary screen of positive knockout colonies (Figure S3A). Human iPSC clone-2 (referred to as ELMSAN1-KO hereafter), which harbors a 1-base pair insertion causing an immediate stop codon, was selected and further validated by

Figure 2. *ELMSAN1* depletion suppresses the contractile and calcium-associated gene expression in hiPSC-CMs.
A through **C**, Relative mRNA expression of (**A**) *TNNI3*, *ACTC1*, *MYH6*; (**B**) *RYR2*, *ATP2A2*, *CACNA1C*, *PLN*; (**C**) *SLC8A1*, *KCNJ2*, *GJA1*, *CDH2* in control and ELMSAN1-KD samples collected at differentiation Day 0 and Day 9 (n=3). (**D**) Coimmunofluorescence staining for cardiac troponin T (green), DAPI (blue), and calcium-handling associated markers SERCA, N-Cadherin, or Kir2.1 in control and ELMSAN1-KD hiPSC-CMs. Quantification results were normalized to cell number (n=18). Data are expressed as mean±SEM (**A** through **C**, 2-way ANOVA; **D**, Student *t* test), ****P<0.0001. *ACTC1* indicates actin alpha cardiac muscle 1; *ATP2A2*, ATPase sarcoplasmic/endoplasmic reticulum Ca^{2+} transporting 2; *CACNA1C*, calcium voltage-gated channel subunit alpha1 C; *CDH2*, cadherin 2; cTnT, cardiac troponin T; ELMSAN1, ELM2-SANT domain-containing scaffolding protein 1; ELMSAN1-KD, ELM2-SANT domain-containing scaffolding protein 1 knockdown; *GJA1*, gap junction protein alpha 1; hiPSC-CM, employed human-induced pluripotent stem cell cardiomyocyte; *KCNJ2*, potassium inwardly-rectifying channel subfamily J member 2; *MYH6*, cardiac alpha myosin heavy chain; *PLN*, phospholamban; RYR2, calcium handling-related markers ryanodine receptor 2; *SLC8A1*, solute carrier family 8 member A1; and *TNNI3*, cardiomyocyte maturation markers cardiac troponin I.

Sanger sequencing (Figure S3B), Western blot analysis (Figure 5A), and morphological analysis (Figure S3C). Consistent with knockdown, ELMSAN1-KO resulted in less efficient cardiac differentiation and reduced cell sizes, as evidenced by decreased expression of cTnT and a lower forward scatter area distribution measured by flow cytometry (Figure 5B). We also examined mRNA expression of additional contractile genes (*ACTC1*, *MYH6*) and calcium-sensitive genes (*PLN*, *SLC8A1*, and *RYR2*) in the ELMSAN1-KO groups, revealing a consistent decrease compared with the WT group (Figure 5C). Immunostaining of cTnI and α-Actinin showed smaller cell sizes and less aligned Z-line structures in *ELMSAN1* null hiPSC-CMs (Figure 5D). The immaturity of ELMSAN1-KO hiPSC-CMs was further demonstrated by the reduced protein expression of SERCA, N-Cadherin, and Kir2.1 (Figure 5E and 5F) and the impaired calcium transients (Figure 5G). More important, the MEA analysis consistently showed disruption in electrical and beating activities in WT and

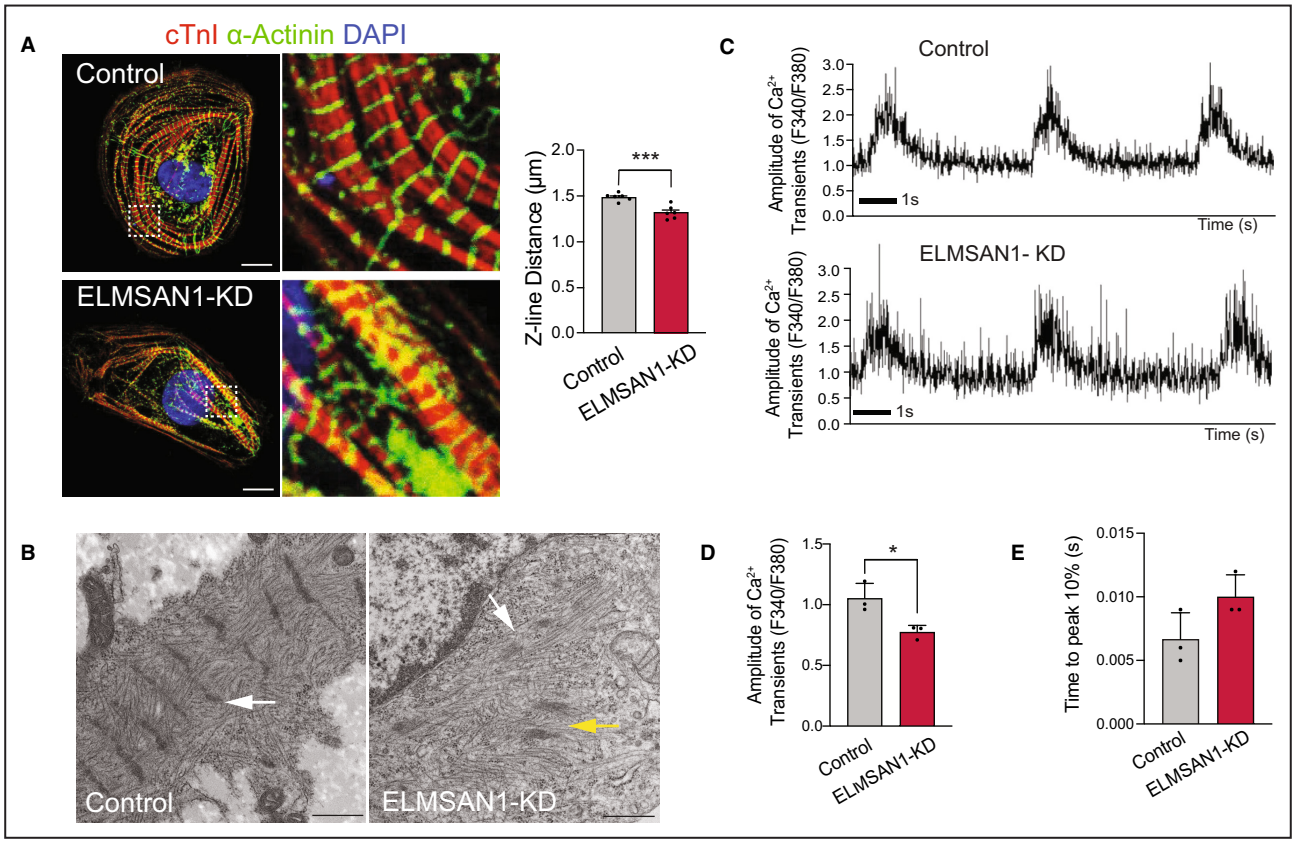

Figure 3. *ELMSAN1* depletion impairs the sarcomere structure and calcium handling properties.
A, Immunofluorescence staining for sarcomere proteins cardiac troponin I (red) and alpha-Actinin (green). Scale bar=10 μm; and the measurement of Z-line distance (μm) was shown in right panel (n=6). **B**, Transmission electron microscopy images of control and ELMSAN1-KD. Scale bar=600 nm. **C**, Recorded traces of calcium transients in control and ELMSAN1-KD hiPSC-CMs. **D** through **E**, Quantification results of amplitude calcium transients and (**E**) time to peak 10%. The calcium transient results were single cell-based analysis (n=3). Data are expressed as mean±SEM (**A**, **D**, and **E**, Student *t* test). *P<0.05, ****P<0.0001. cTnI indicates cardiac troponin I; ELMSAN1, ELM2-SANT domain-containing scaffolding protein 1; ELMSAN1-KD, ELM2-SANT domain-containing scaffolding protein 1 knockdown; and hiPSC-CM, employed human-induced pluripotent stem cell cardiomyocyte.

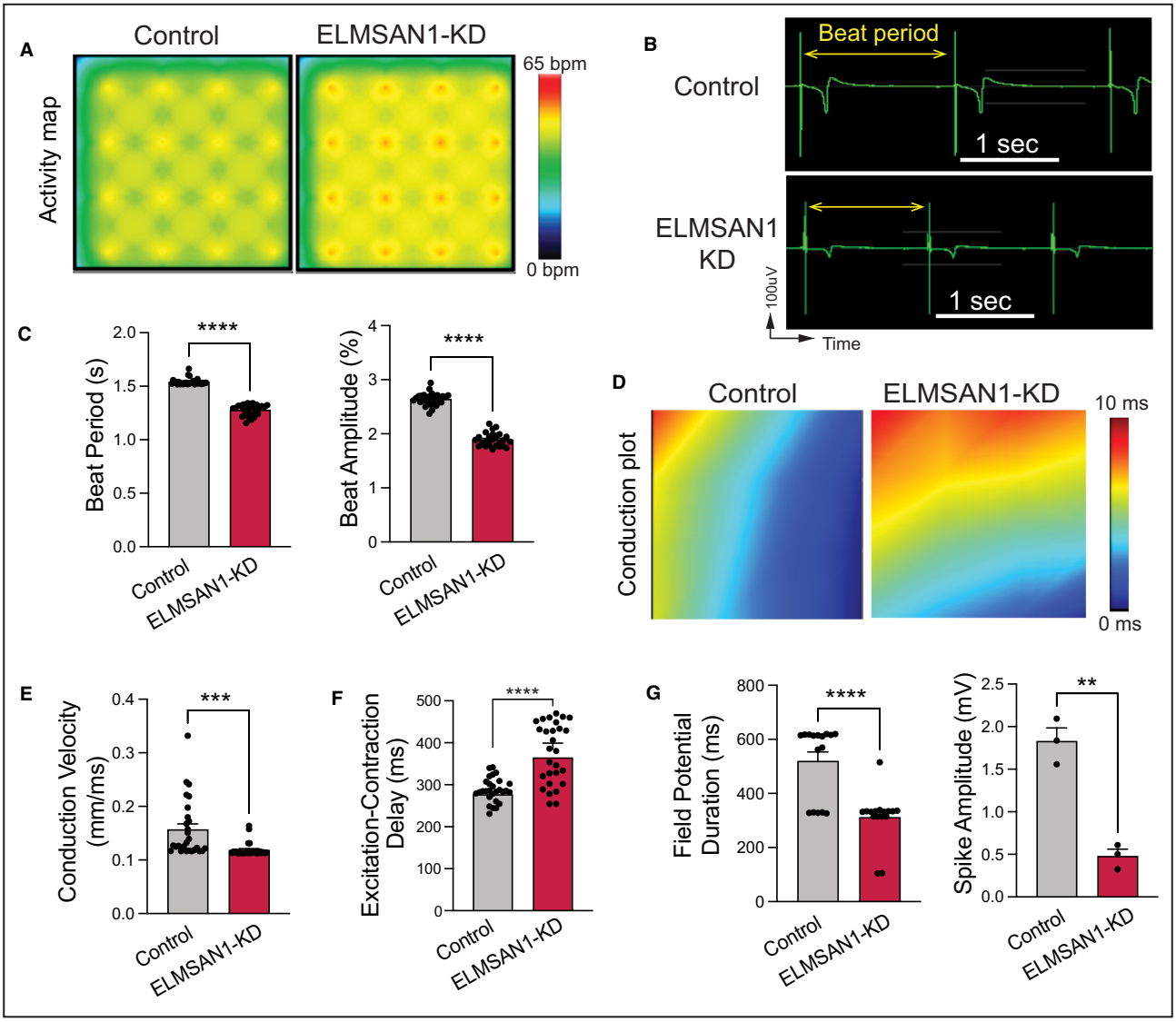

Figure 4. Microelectrode array analysis shows electrophysiology immaturity in cardiomyocytes derived from *ELMSAN1*-depleted hiPSCs.

A, Activity maps show a higher rate in the ELMSAN-KD hiPSC-CMs. **B**, Representative field potential recordings are displayed for hiPSC-CMs from control and ELMSAN1-KD group. **C**, Field potential recordings were used for calculation of beat period and beat amplitude (n=28). **D**, Conduction plot shows propagation delay in ELMSAN1-KD CMs; blue region represents origin of beat (start electrode). Different colors show propagation delay time as shown in scale bar. **E** and **F**, Quantification of (**E**) max propagation (difference in beat detection time between electrodes in a well) and (**F**) conduction velocity in samples as indicated (n=28). **G**, Field potential duration (n=16) and spike amplitude (n=3) were analyzed in control and ELMSAN1-KD groups. Data are expressed as mean±SEM (**C** through **G**, Student *t* test). **P*<0.05, ***P*<0.01, *****P*<0.0001. ELMSAN1 indicates ELM2-SANT domain-containing scaffolding protein 1; ELMSAN1-KD, ELM2-SANT domain-containing scaffolding protein 1 knockdown; hiPSC-CM, employed human-induced pluripotent stem cell cardiomyocyte; ms, millisecond; m/s, meter per second; and s, second.

ELMSAN1-KO iPSC-CMs (Table), supporting the notion that ELMSAN1 is required for the functional maturation of cardiomyocytes.

Transcriptomic Analysis Demonstrated Cardiac-Specific Impact of ELMSAN1 on Gene Expression

Next, to advance our understanding of ELMSAN1's molecular effects on hiPSCs and cardiomyocytes, we performed RNA sequencing (RNA-seq) analysis on WT and KO cells collected at differentiation Day 0 and Day 9. Principal component analysis revealed that the variance between Day 0 WT hiPSCs and Day 0 KO hiPSCs was significantly smaller than that between Day 9 WT hiPSC-CMs and Day 9 KO hiPSC-CMs, indicating that ELMSAN1-KO has a less pronounced effect on overall gene expression in hiPSCs compared with that of hiPSC-CMs (Figure S4A). The volcano plot demonstrated that only 479 differentially expressed genes

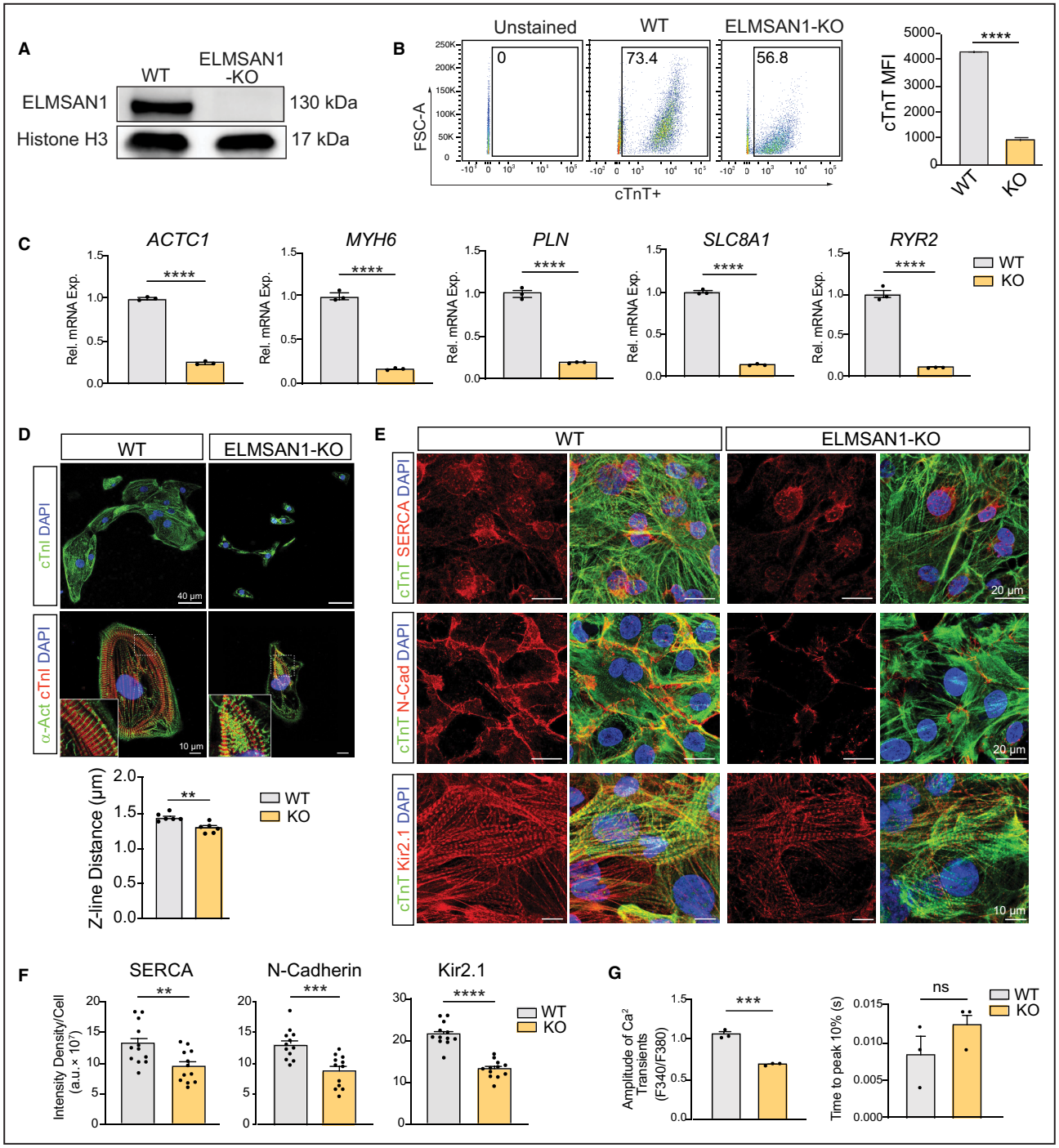

Figure 5. ***ELMSAN1*** **knockout results in similar defects in hiPSC-CMs.**
A, Western blotting of ELMSAN1 in wild-type hiPSCs and the ELMSAN1-KO stable line. Histone 3 is used as an internal control. **B**, Flow cytometry analysis for differentiation efficiency based on cardiac troponin T expression on Day 9. The MFI was quantified (n=3). **C**, RT-qPCR analysis of genes associated with contractility and calcium handling in hiPSC-CMs with or without ELMSAN1 (n=3). **D**, Confocal images and quantifications show cell size, sarcomere alignment, and Z-distance as labeled with cardiac troponin I and alpha-Actinin in WT and KO hiPSC-CMs (n=6). Scale bar=10 μm. **E** and **F**, Immunofluorescence analysis of calcium-handling associated markers, including SERCA, N-Cadherin, and Kir2.1 (n=12). Scale bar=10 μm. **G**, Trace of calcium transients were analyzed for amplitude and time to peak 10% in WT and KO samples. The results were single cell-based analysis (n=3). Data are expressed as mean±SEM (**B**, **C**, **D**, **F**, and **G**, Student *t*-test). **P*<0.05, ***P*<0.01, ****P*<0.001, *****P*<0.0001. cTnT indicates cardiac troponin T; ELMSAN1, ELM2-SANT domain-containing scaffolding protein 1; ELMSAN1-KO, ELM2-SANT domain-containing scaffolding protein 1 knockout; FSC-A, forward scatter area; hiPSC-CM, employed human-induced pluripotent stem cell cardiomyocyte; MFI, median fluorescence intensity; ms, milliseconds; m/s, meters per second; RT-qPCR, reverse transcription quantitative polymerase chain reaction; s, second; and WT, wild type.

MEA Measurements in WT and ELMSAN1 KO iPSC-CMs

MEA measurements	WT (Mean±SEM)	KO (Mean±SEM)	FC (KO/WT)	n (WT, KO)	*P* value (WT vs KO)
Beat period	2.45±0.02	2.19±0.02	0.89	(30)	7.93E-07
Beat amplitude	2.87±0.06	1.16±0.03	0.40	(30)	2.45E-26
Excitation-contraction delay	310.88±18.26	412.82±32.10	1.33	(29)	4.18E-03
Maximum propagation delay	8.69±0.10	10.02±0.04	1.15	(28, 29)	3.13E-14
Conduction velocity	0.15±0.00	0.13±0.00	0.89	(30)	4.62E-08
Field potential duration	544.54±20.51	244.98±18.15	0.45	(30)	6.16E-16
Spike amplitude	1.71±0.02	0.73±0.02	0.43	(30)	2.37E-40

ELMSAN1-KO indicates ELM2-SANT domain-containing scaffolding protein 1 knockout; FC, fold change; MEA, microelectrode array; and WT, wild type.

(log_2 fold change >1, $P<0.05$) were identified between the Day 0 KO and the Day 0 WT groups, whereas a substantial number of 5437 coding genes exhibited significant alterations upon ELMSAN1-KO in hiPSC-CMs (Figure S4B). This differential gene regulation might be associated with the distinct expression levels of MiDAC components. We thus determined the dynamic expression of ELMSAN1, DNTTIP1, and HDAC1 proteins at different time points along the differentiation process in WT cells. Interestingly, ELMSAN1 was highly expressed in WT hiPSC-CMs whereas DNTTIP1 and HDAC1 were altered initially but returned to a hiPSC-comparable level in cardiomyocytes (Figure 6A and 6B). In addition, we tested whether *ELMSAN1* knockout differentially affects DNTTIP1 and HDAC1 expression in WT and mutant cells. The results showed that *ELMSAN1* deletion did not alter protein levels of other components (Figure S4C). Given MiDAC's major role in histone deacetylation, we further hypothesized that ELMSAN1 might regulate global histone acetylation levels in a cell-type-specific manner. To investigate this, we assessed the levels of H3K9/K14/K27ac, known MiDAC substrates in vitro.[33] As demonstrated, H3K9ac and H3K14ac levels remained largely unchanged during cardiac differentiation of WT or KO hiPSCs (Figure 6C). In contrast, the well-known enhancer mark H3K27ac decreased along differentiation and, surprisingly, was further reduced in ELMSAN1-KO hiPSC-CMs but not in hiPSCs (Figure 6C). Although this suggests an indirect regulation of MiDAC on H3K27ac, the decreased level of H3K27ac might be associated with impaired cardiac gene activation. Additionally, we examined a panel of stage-specific lineage markers and consistently demonstrated the repression of cardiac lineage due to the loss of *ELMSAN1* (Figure S4D). *BMP4* is among the top genes that are specifically activated in ELMSAN1-KO hiPSC-CMs (Figure 6D), potentially impeding cardiomyocyte development during the cardiac maturation stage as previously reported.[34] As evidenced by the chromatin immunoprecipitation-qPCR results, an increased level of H3K27ac at the *BMP4* promoter region was found in ELMSAN1-KO hiPSC-CMs (Figure 6E). Our findings thus reveal a cell-type-specific role of ELMSAN1 in modulating histone acetylation and gene expression.

To comprehensively understand transcriptomic changes across all samples, we first selected the top 1000 genes displaying the highest variance for a K-means clustering analysis. These genes were subsequently categorized into 5 clusters based on their expression patterns (Figure 6F). In particular, Cluster A, which consists of genes associated with stem cell properties, showed high expression levels in Day 0 hiPSCs. Conversely, Cluster E genes, related to heart development, were predominantly expressed in D9 hiPSC-CMs. ELMSAN1 expression levels led to minimal alteration on genes in Cluster A and E. Cluster B genes (N=239) demonstrated an interesting

Figure 6. Cardiac-specific impact of ELMSAN1 on gene expression.
A and **B**, Western blot analysis and quantification (**B**) of ELMSAN1, DNTTIP1, and HDAC1 expression along hiPSC cardiac differentiation. All bands were normalized to GAPDH (n=2). **C**, Western blotting and quantification of histone H3K14ac, H3K27ac, and H3K9ac in samples as indicated (n=3). **D**, RT-qPCR analysis of *BMP4* expression at differentiation Days 0, 3, and 9 from WT or ELMSAN1-KO hiPSCs (n=3). **E**, ChIP-qPCR analysis shows the level of H3K27ac at the *BMP4* promoter region in WT and ELMSAN1-KO hiPSC-CMs (n=3). **F**, Heatmap for K-means clustering of the top 1000 genes with highest variance across the 4 groups. Right panel: top Gene Ontology of biological processes significantly enriched in each cluster. Number of genes is listed. **G** and **H**, Enriched GO terms associated with (**G**) upregulated or (**H**) downregulated genes in D9 KO samples when compared with D9 WT samples. Data are expressed as mean±SEM (**C**, Student *t* test; **D**, 1-way ANOVA; **E**, 2-way ANOVA). ***P*<0.01, *****P*<0.0001. ChIP indicates chromatin immunoprecipitation; DNTTIP1, deoxynucleotidyltransferase terminal interacting protein 1; ELMSAN1, ELM2-SANT domain-containing scaffolding protein 1; ELMSAN1-KO, ELM2-SANT domain-containing scaffolding protein 1 knockout; GO, gene ontology; HDAC1, histone deacetylase 1; hiPSC-CM, employed human-induced pluripotent stem cell cardiomyocyte; RT-qPCR, reverse transcription quantitative polymerase chain reaction; and WT, wild type.

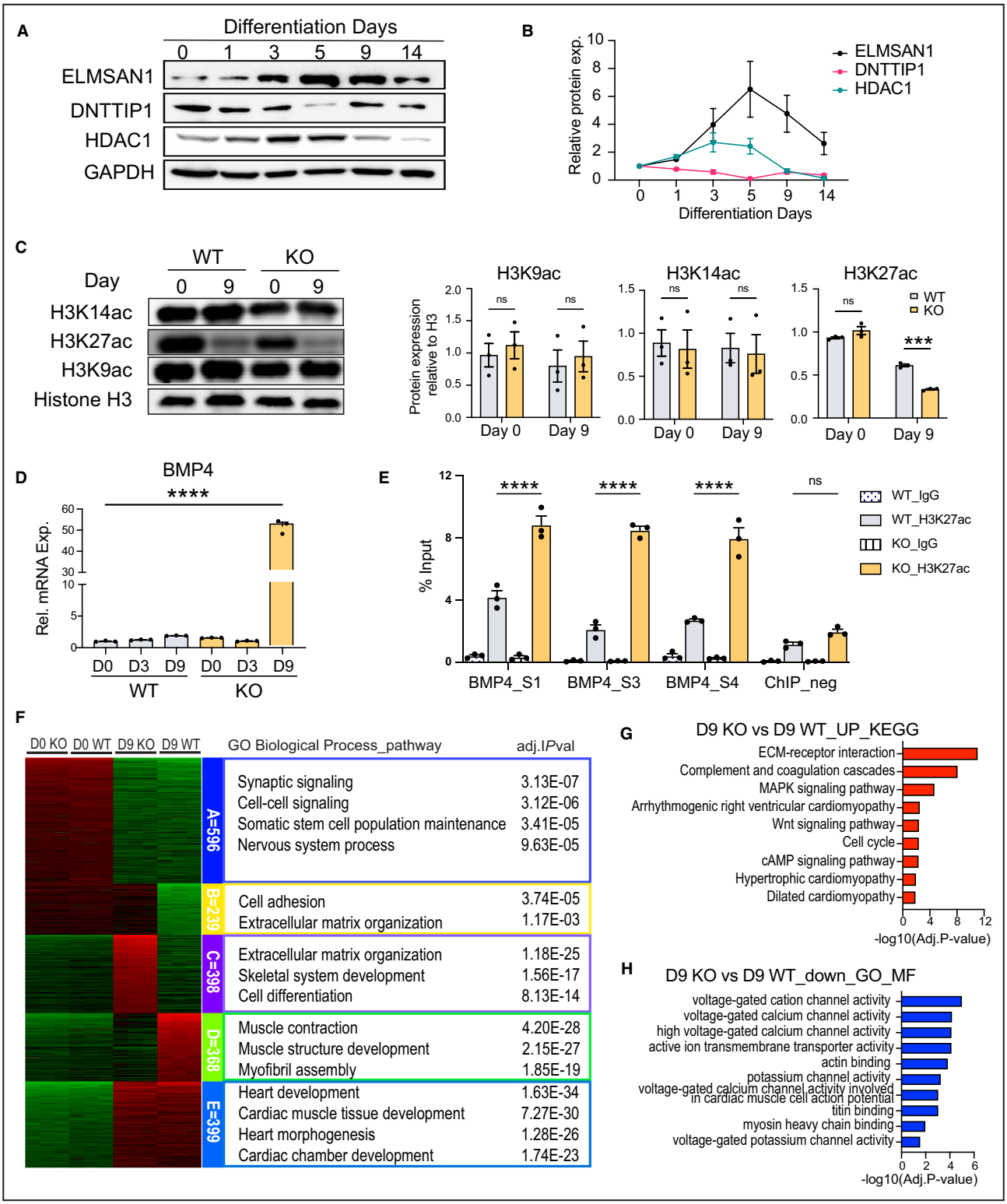

expression pattern: they are uniquely downregulated in WT-hiPSC-CMs and associated with "cell adhesion" and "extracellular matrix organization," suggesting that loss of ELMSAN1 leads to an incomplete exit of pluripotency status lingering from stem cells. Cluster C highlighted genes uniquely upregulated upon ELMSAN1-KO in hiPSC-CMs, associated with "extracellular matrix organization," skeletal system development, and cell differentiation. Direct comparison of Day 9 KO and Day 9 WT samples uncovered further pathways enriched in ELMSAN1-KO hiPSC-CMs, such as MAPK signaling pathway and cell cycle

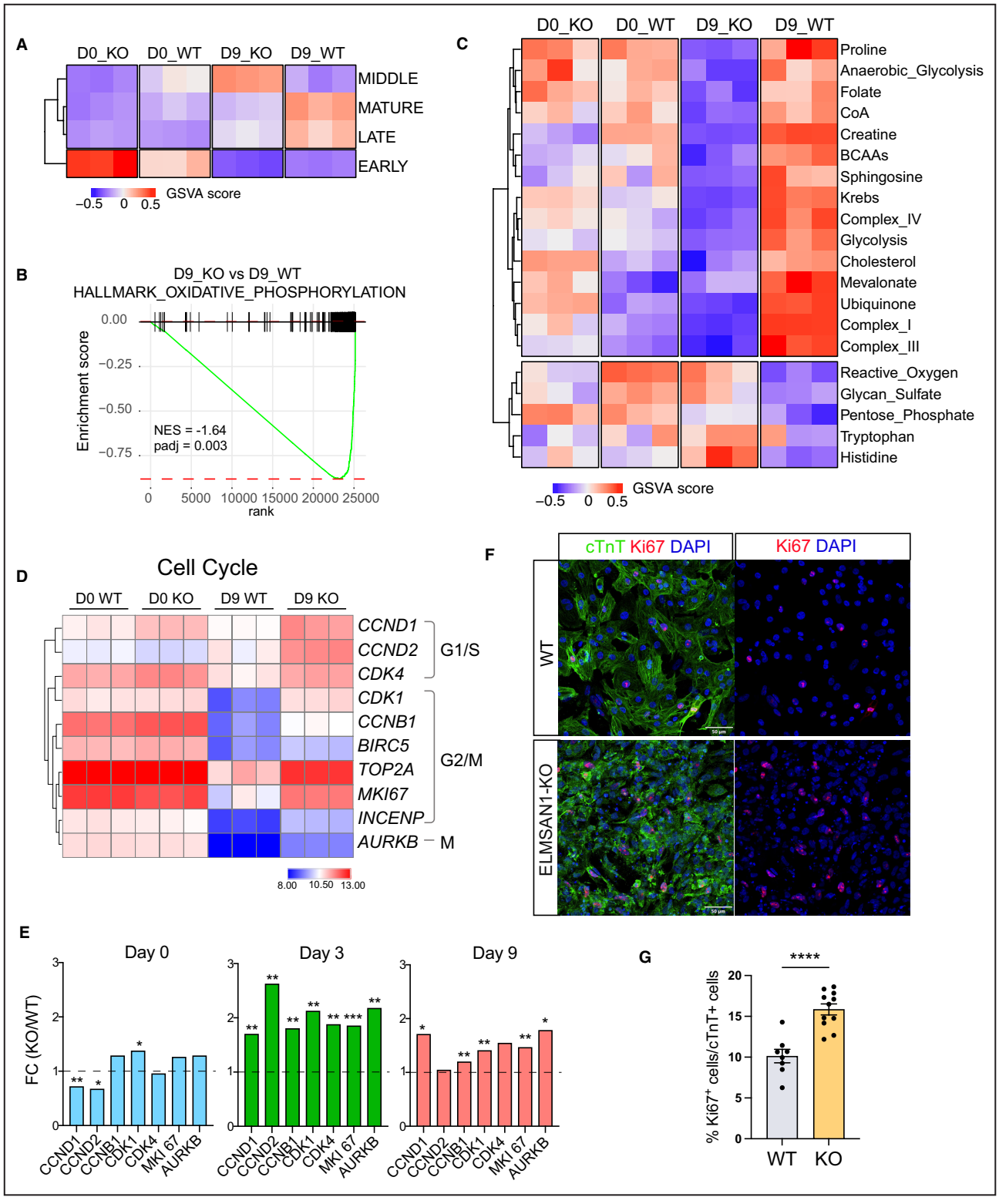

(Figure 6G). Additionally, Cluster D genes, uniquely expressed in WT hiPSC-CMs, were related to muscle contraction, muscle structure development, and myofibril assembly. Differentially expressed genes between Day 9 KO and WT samples underscored a reduced expression of genes involved in ion channels and sarcomere component binding in ELMSAN1-KO hiPSC-CMs (Figure 6H), supporting our previous notion that ELMSAN1 is required for the functional maturation of hiPSC-CMs.

Figure 7. Disrupted metabolism and enhanced cell proliferation in *ELMSAN1*-null hiPSC-CMs.
A, Heatmap shows enrichment of gene sets associated with cardiomyocyte maturation stages as determined by GSVA. **B**, GSEA enrichment plot displays gene set associated with oxidative phosphorylation in comparison of Day 9 KO and Day 9 WT samples. **C**, Heatmap generated from GSVA scores shows enrichment of metabolism-related pathways in WT and KO samples. **D**, Heatmap shows expression alteration of cell cycle genes in cardiomyocytes but not iPSCs following *ELMSAN1* knockout. **E**, qPCR analysis presents FC of cycling gene mRNA expression (ELMSAN1-KO vs WT) at cardiac differentiation Days 0, 3, and 9. **F**, Representative immunofluorescence staining of cTnT (green) and Ki67 (red) in purified cardiomyocytes derived from ELMSAN1-KO and WT hiPSCs. Scale bar=10 μm. **G**, Quantification of (**F**) defined Ki67+ percentage out of cTnT+ cells (n≥8). Data are presented as mean±SEM (**E**, 1-way ANOVA; **G**, Student *t* test). **P*<0.05, ***P*<0.01, ****P*<0.001, *****P*<0.0001. cTnT indicates cardiac troponin T; ELMSAN1, ELM2-SANT domain-containing scaffolding protein 1; ELMSAN1-KO, ELM2-SANT domain-containing scaffolding protein 1 knockout; FC, fold change; GSEA, gene set enrichment analysis; GSVA, gene set variation analysis; HDAC1, histone deacetylase 1; hiPSC-CM, employed human-induced pluripotent stem cell cardiomyocyte; RT-qPCR, reverse transcription quantitative polymerase chain reaction; and WT, wild type.

Dysregulated Metabolism Genes and Cell Proliferation Were Identified in ELMSAN1-KO hiPSC-CMs

Further gene set enrichment analysis elucidated the immature status of cardiomyocytes derived from ELMSAN1-KO hiPSC compared with WT hiPSC. Previously reported gene sets representing early, middle, late, and mature stages during cardiomyocyte maturation[26] were used for the gene set variation analysis. The results, visualized in a heatmap plot (Figure 7A), showed decreased expression of genes from the late and mature stages but increased middle-stage genes in ELMSAN1-KO hiPSC-CMs, suggesting a delayed maturation caused by loss of *ELMSAN1*. In particular, a panel of genes involved in calcium handling, ion channels, and sarcomere structure were largely suppressed (Figure S4E and S4F). Moreover, changes in energy metabolism serve as another hallmark feature of cardiomyocyte maturation, characterized by increases in fatty acid oxidation and oxidative phosphorylation.[35] Gene set enrichment analysis suggested that ELMSAN1-KO hiPSC-CMs exhibited decreased expression of oxidative phosphorylation genes (Figure 7B). Additional gene enrichment analysis showed reduced gene signatures of most metabolite pathways in the ELMSAN1-KO hiPSC-CMs, suggesting that the *ELMSAN1* null hiPSC-CMs had a reduced energy production that often occurs in heart failure (Figure 7C).[36] Besides the metabolic switch, cardiomyocyte functional maturation is concurrent with the inhibition of cell proliferation.[35] From our transcriptome data, we found upregulation of various cell cycle regulators, such as cyclins D1/D2/B1 and cyclin-dependent kinase 1 and 4, only in KO hiPSC-CMs (Figure 7D). The changes did not happen in hiPSCs but began to emerge at early differentiation Day 3 and sustained to Day 9 (Figure 7E). To determine cell proliferation changes upon *ELMSAN1* loss specifically in cardiomyocytes rather than other cells derived during differentiation, we enriched hiPSC-CMs with lactate selection[37] and evaluated the expression of proliferation markers, Ki67 and PH3, in cTnT+ cardiomyocytes (Figure 7F and 7G; Figure S4G). A higher percentage of Ki67 or PH3 was found in the ELMSAN1-KO cardiomyocytes. These findings reveal that the cardiac-specific role of ELMSAN1 is likely associated with molecular and cellular changes associated with metabolism and cell proliferation.

DISCUSSION

The MiDAC complex remains one of the most underexplored class I histone deacetylase complexes, with its contributions to embryonic development and physiologically relevant functions yet to be slightly elucidated. This study marks a pioneering work focusing on the role of ELMSAN1, a component of MiDAC, in the differentiation and maturation of cardiomyocytes derived from hiPSCs. We employed both shRNA-mediated knockdown and CRISPR/Cas9-based knockout approaches to deplete *ELMSAN1*, observing a consequent reduction in cardiac differentiation. In particular, *ELMSAN1* loss led to a variety of changes in cardiomyocyte characteristics, such as delayed exit of the pluripotent stage, reduced expression of cardiac lineage genes, disorganization of sarcomere structures, and impaired electrophysiological and calcium handling properties, collectively contributing to the immaturity of the hiPSC-derived cardiomyocytes.

Our data showed rare morphology and transcriptome changes in ELMSAN1-KO hiPSCs, indicating that MiDAC may not be essential for maintaining hiPSCs. This finding aligns with previous research in mouse embryonic stem cells, where the depletion of *Elmsan1* or *Dnttip1* had minimal effect on stem cell identity but impaired neuronal differentiation.[25] However, other HDAC1-containing complexes like NuRD and Sin3A are known to be required for regulating self-renewal and pluripotency in stem cells,[38,39] suggesting a potential role of MiDAC in contributing to cell type-specific regulation of the widely expressed-HDAC1. During cardiac differentiation, we observed a delayed exit from pluripotency in *ELMSAN1*-deficient hiPSCs (Figure 1D), consistent with previous findings that HDAC1 inhibition influences differentiation-induced pluripotency reduction and impairs cardiac lineage commitment.[19,40]

Notably, extended culture (>20 days) of ELMSAN1-KD and KO hiPSC-CMs did not alleviate the impaired electrophysiological properties of ELMSAN1 deficient cardiomyocytes (data not shown). Furthermore, we found increased expression of ELMSAN1 and DNTTIP1 during mesoderm differentiation and cardiac lineage commitment (Figure 6A). This observation may be associated with the phenotype seen in mice where germline knockout of *Elmsan1* or *Dnttip1* led to embryonic lethality at E16.5.[23] Nevertheless, to gain a deeper understanding of MiDAC's role in embryonic heart development, further investigation using conditional knockout mice is warranted.

HDACs widely act on both actively transcribed and repressed genes to reshape the chromatin landscape, leading to subsequent complex-dependent transcriptional outcomes.[41] Each HDAC complex exhibits diverse functions due to variable assemblies and diverse components. The 3 major HDAC1/2-containing protein complexes—CoREST, NuRD, and SIN3A—play pivotal roles in various cell fate decisions, including cardiac differentiation.[42] For instance, LSD1 (lysine-specific histone demethylase 1A), a component of SIN3A complex, has been reported to have cell type-specific functions in cardiac fibroblast activation and cardiomyocyte dysfunction in adult heart homeostasis and injury response.[43] The CHD4 (chromodomain-helicase-DNA-binding protein 4)-containing NuRD complex plays a crucial role in maintaining the functional identity of cardiac muscles.[44] However, the function of many other subunits in these complexes remains unclear. Because HDAC1 and HDAC2 participate in multiprotein transcriptional complexes, a loss of function study would be helpful to provide insights into the specific function of individual complexes. Our study, with a focus on ELMSAN1, indicates the potential role of MiDAC in cardiac differentiation and maturation for the first time, offering alternative targets for complex-specific HDAC inhibition in the heart. As cardiomyocyte maturation changes are observed in several heart disorders such as cardiomyopathy, hypertrophy, and heart failure, our findings also indicate that MiDAC may play an important role in certain heart pathological conditions. Interestingly, ELMSAN1 has been reported as one of the top genes associated with a trait of cardiac remodeling based on the data from the Framingham Heart Study.[45] Our preliminary genome-wide association study showed an association of DNTTIP1 with cardiomyopathy (data not shown). Future investigations of MiDAC in diseased conditions are likely to provide valuable mechanistic insights into heart disease pathogenesis.

Still, the molecular details about how MiDAC regulates gene expression through deacetylation mechanisms remain unclear. A loss of MiDAC function in mouse embryonic stem cells resulted in bulk increase of H4K20ac but reduced H3K27ac, supporting the downregulation of neural genes during differentiation.[25] Although their further study showed that H4K20ac is directly regulated by MiDAC and antagonizes the role of MLL3/4 (mixed lineage leukemia 3/4) complexes on genomic regulatory elements,[24] it is still unknown how H3K27ac is regulated by MiDAC. Our results also showed significant reduction of H3K27ac levels after *ELMSAN1* depletion. The possible underlying mechanisms might be associated with the perturbation of HDAC1 activity among different complexes or redistribution of histone acetylation on specific regulatory loci. MiDAC may also target non-histone proteins like other HDAC1 complexes. One of the ELMSAN1 paralogs, RCOR1 (also known as CoREST), serves as a scaffold component of CoREST HDAC1-containing complex, which is involved in a noncanonical mechanism associated with RNA polymerase II deacetylation to inhibit transcription elongation.[46] Future studies in these directions may provide insightful mechanistic details about MiDAC.

CONCLUSIONS

In conclusion, this study represents the first to present direct evidence of the cardiac-specific role of ELMSAN1 in the process of hiPSC cardiomyocyte differentiation and maturation. Our findings conclusively establish that an additional HDAC Class I complex, MiDAC, plays critical roles in cardiomyocyte differentiation involved in regulating sarcomere structure formation, calcium handling, and electrophysiological properties.

ARTICLE INFORMATION

Received January 31, 2024; accepted May 23, 2024.

Affiliations

Department of Biomedical Engineering, Heersink School of Medicine, School of Engineering (Y-A.L., J.S., L.W., M.W., Y.W., A.G., R.C.M., H.L., W.G.P., J.Z., Y.Z.), Department of Medicine, Division of Cardiovascular Disease, Heersink School of Medicine (J.Z.), Department of Medicine, Division of Hematology/Oncology, Heersink School of Medicine (R.L.) and O'Neal Comprehensive Cancer Center, University of Alabama at Birmingham, Birmingham, AL (R.L.).

Acknowledgments

Yu-An Lu and Jiacheng Sun designed experiments, conducted the experiments, analyzed the data, prepared figures, and wrote the article; Lu Wang, Meimei Wang, Yalin Wu, Anteneh Getachew, and Hui Li conducted experiments; Rachel C. Matthews and William Gao Peng analyzed data and prepared the figures; Jianyi Zhang provided technical and financial support; Rui Lu analyzed the sequencing data and revised the article; Yang Zhou supervised the project, designed the experiments, analyzed the data, prepared the figures, and wrote the article.

Sources of Funding

This work was supported in part by National Institutes of Health: R01 HL153220 (Y.Z.), R01 CA259480 (R.L.), R01 HL149137 (J.Z.), and PO1 HL160476 (Jianyi Zhang); by The Mark Foundation for Cancer Research (R. L.); and by American Heart Association: Transformational Project Award 969529 (Y.Z.), Predoctoral Fellowship Award 23PRE1025367 (J.S.) and

23PRE1027112 (M.W.), Postdoctoral Fellowship Award 24POST1188989 (A.G.). R.L. is an American Society of Hematology Scholar in Basic Science and a Research Scholar of American Cancer Society (RSG-22-036-01-DMC).

Disclosures

None.

Supplemental Material

Tables S1–S4
Figures S1–S4
Video S1
Video S2

REFERENCES

1. Brand T. Heart development: molecular insights into cardiac specification and early morphogenesis. *Dev Biol*. 2003;258:1–19. doi: 10.1016/S0012-1606(03)00112-X
2. Buckingham M, Meilhac S, Zaffran S. Building the mammalian heart from two sources of myocardial cells. *Nat Rev Genet*. 2005;6:826–835. doi: 10.1038/nrg1710
3. Srivastava D. Making or breaking the heart: from lineage determination to morphogenesis. *Cell*. 2006;126:1037–1048. doi: 10.1016/j.cell.2006.09.003
4. Linglart L, Bonnet D. Epigenetics and congenital heart diseases. *J Cardiovasc Dev Dis*. 2022;9:9. doi: 10.3390/jcdd9060185
5. Lim TB, Foo SYR, Chen CK. The role of epigenetics in congenital heart disease. *Genes (Basel)*. 2021;12:390. doi: 10.3390/genes12030390
6. Lee J, Shao NY, Paik DT, Wu H, Guo H, Termglinchan V, Churko JM, Kim Y, Kitani T, Zhao MT, et al. SETD7 drives cardiac lineage commitment through stage-specific transcriptional activation. *Cell Stem Cell*. 2018;22:428–444. doi: 10.1016/j.stem.2018.02.005
7. Burridge PW, Sharma A, Wu JC. Genetic and epigenetic regulation of human cardiac reprogramming and differentiation in regenerative medicine. *Annu Rev Genet*. 2015;49:461–484. doi: 10.1146/annurev-genet-112414-054911
8. Lan Y, Evans T. Epigenetic regulation of cardiac development and disease through DNA methylation. *J Life Sci*. 2019;1:1–10. doi: 10.36069/JoLS/20190901
9. Gujral P, Mahajan V, Lissaman AC, Ponnampalam AP. Histone acetylation and the role of histone deacetylases in normal cyclic endometrium. *Reprod Biol Endocrinol*. 2020;18:84. doi: 10.1186/s12958-020-00637-5
10. Cavalieri V. The expanding constellation of histone post-translational modifications in the epigenetic landscape. *Genes (Basel)*. 2021;12:1596. doi: 10.3390/genes12101596
11. Bannister AJ, Kouzarides T. Regulation of chromatin by histone modifications. *Cell Res*. 2011;21:381–395. doi: 10.1038/cr.2011.22
12. Gonneaud A, Turgeon N, Jones C, Couture C, Lévesque D, Boisvert F-M, Boudreau F, Asselin C. HDAC1 and HDAC2 independently regulate common and specific intrinsic responses in murine enteroids. *Sci Rep*. 2019;9:5363. doi: 10.1038/s41598-019-41842-6
13. Yang XJ, Seto E. The Rpd3/Hda1 family of lysine deacetylases: from bacteria and yeast to mice and men. *Nat Rev Mol Cell Biol*. 2008;9:206–218. doi: 10.1038/nrm2346
14. Millard CJ, Watson PJ, Fairall L, Schwabe JWR. Targeting class I histone deacetylases in a "complex" environment. *Trends Pharmacol Sci*. 2017;38:363–377. doi: 10.1016/j.tips.2016.12.006
15. Yang JY, Wang Q, Wang W, Zeng LF. Histone deacetylases and cardiovascular cell lineage commitment. *World J Stem Cells*. 2015;7:852–858. doi: 10.4252/wjsc.v7.i5.852
16. Lagger G, O'Carroll D, Rembold M, Khier H, Tischler J, Weitzer G, Schuettengruber B, Hauser C, Brunmeir R, Jenuwein T, et al. Essential function of histone deacetylase 1 in proliferation control and CDK inhibitor repression. *EMBO J*. 2002;21:2672–2681. doi: 10.1093/emboj/21.11.2672
17. Dovey OM, Foster CT, Cowley SM. Histone deacetylase 1 (HDAC1), but not HDAC2, controls embryonic stem cell differentiation. *Proc Natl Acad Sci USA*. 2010;107:8242–8247. doi: 10.1073/pnas.1000478107
18. Montgomery RL, Davis CA, Potthoff MJ, Haberland M, Fielitz J, Qi X, Hill JA, Richardson JA, Olson EN. Histone deacetylases 1 and 2 redundantly regulate cardiac morphogenesis, growth, and contractility. *Genes Dev*. 2007;21:1790–1802. doi: 10.1101/gad.1563807
19. Hoxha E, Lambers E, Xie H, De Andrade A, Krishnamurthy P, Wasserstrom JA, Ramirez V, Thal M, Verma SK, Soares MB, et al. Histone deacetylase 1 deficiency impairs differentiation and electrophysiological properties of cardiomyocytes derived from induced pluripotent cells. *Stem Cells*. 2012;30:2412–2422. doi: 10.1002/stem.1209
20. Kim JY, Shen S, Dietz K, He Y, Howell O, Reynolds R, Casaccia P. HDAC1 nuclear export induced by pathological conditions is essential for the onset of axonal damage. *Nat Neurosci*. 2010;13:180–189. doi: 10.1038/nn.2471
21. Pagliuca FW, Collins MO, Lichawska A, Zegerman P, Choudhary JS, Pines J. Quantitative proteomics reveals the basis for the biochemical specificity of the cell-cycle machinery. *Mol Cell*. 2011;43:406–417. doi: 10.1016/j.molcel.2011.05.031
22. Itoh T, Fairall L, Muskett FW, Milano CP, Watson PJ, Arnaudo N, Saleh A, Millard CJ, El-Mezgueldi M, Martino F, et al. Structural and functional characterization of a cell cycle associated HDAC1/2 complex reveals the structural basis for complex assembly and nucleosome targeting. *Nucleic Acids Res*. 2015;43:2033–2044. doi: 10.1093/nar/gkv068%JNucleicAcidsResearch
23. Turnbull RE, Fairall L, Saleh A, Kelsall E, Morris KL, Ragan TJ, Savva CG, Chandru A, Millard CJ, Makarova OV, et al. The MiDAC histone deacetylase complex is essential for embryonic development and has a unique multivalent structure. *Nat Commun*. 2020;11:3252. doi: 10.1038/s41467-020-17078-8
24. Wang X, Rosikiewicz W, Sedkov Y, Mondal B, Martinez T, Kallappagoudar S, Tvardovskiy A, Bajpai R, Xu B, Pruett-Miller SM, et al. The MLL3/4 complexes and MiDAC co-regulate H4K20ac to control a specific gene expression program. *Life Sci Alliance*. 2022;5:e202201572. doi: 10.26508/lsa.202201572
25. Mondal B, Jin H, Kallappagoudar S, Sedkov Y, Martinez T, Sentmanat MF, Poet GJ, Li C, Fan Y, Pruett-Miller SM, et al. The histone deacetylase complex MiDAC regulates a neurodevelopmental gene expression program to control neurite outgrowth. *eLife*. 2020;9:e57519. doi: 10.7554/eLife.57519
26. Zhou Y, Wang L, Liu Z, Alimohamadi S, Yin C, Liu J, Qian L. Comparative gene expression analyses reveal distinct molecular signatures between differentially reprogrammed cardiomyocytes. *Cell Rep*. 2017;20:3014–3024. doi: 10.1016/j.celrep.2017.09.005
27. Possemato R, Marks KM, Shaul YD, Pacold ME, Kim D, Birsoy K, Sethumadhavan S, Woo HK, Jang HG, Jha AK, et al. Functional genomics reveal that the serine synthesis pathway is essential in breast cancer. *Nature*. 2011;476:346–350. doi: 10.1038/nature10350
28. Wang L, Nguyen T, Rosa-Garrido M, Zhou Y, Cleveland DC, Zhang, J. Comparative analysis of the cardiomyocyte differentiation potential of induced pluripotent stem cells reprogrammed from human atrial or ventricular fibroblasts. *Front Bioeng Biotechnol*. 2023;11:1108340. doi: 10.3389/fbioe.2023.1108340
29. Zhao M, Tang Y, Zhou Y, Zhang J. Deciphering role of Wnt Signalling in cardiac mesoderm and cardiomyocyte differentiation from human iPSCs: four-dimensional control of Wnt pathway for hiPSC-CMs differentiation. *Sci Rep*. 2019;9:19389. doi: 10.1038/s41598-019-55620-x
30. Minor AJ, Coulombe KLK. Stimulating calcium handling in hiPSC-derived engineered cardiac tissues enhances force production. *Stem Cells Transl Med*. 2022;11:97–106. doi: 10.1093/stcltm/szab002
31. White MC, Pang L, Yang X. MicroRNA-mediated maturation of human pluripotent stem cell-derived cardiomyocytes: towards a better model for cardiotoxicity? *Food Chem Toxicol*. 2016;98:17–24. doi: 10.1016/j.fct.2016.05.025
32. Qu Y, Vargas HM. Proarrhythmia risk assessment in human induced pluripotent stem cell-derived Cardiomyocytes using the maestro MEA platform. *Toxicol Sci*. 2015;147:286–295. doi: 10.1093/toxsci/kfv128
33. Wang ZA, Millard CJ, Lin CL, Gurnett JE, Wu M, Lee K, Fairall L, Schwabe JW, Cole PA. Diverse nucleosome site-selectivity among histone deacetylase complexes. *elife*. 2020;9:e57663. doi: 10.7554/eLife.57663
34. Kattman SJ, Witty AD, Gagliardi M, Dubois NC, Niapour M, Hotta A, Ellis J, Keller G. Stage-specific optimization of activin/nodal and BMP signaling promotes cardiac differentiation of mouse and human pluripotent stem cell lines. *Cell Stem Cell*. 2011;8:228–240. doi: 10.1016/j.stem.2010.12.008
35. Guo Y, Pu WT. Cardiomyocyte maturation: new phase in development. *Circ Res*. 2020;126:1086–1106. doi: 10.1161/CIRCRESAHA.119.315862

36. Karwi QG, Uddin GM, Ho KL, Lopaschuk GD. Loss of metabolic flexibility in the failing heart. *Front Cardiovasc Med*. 2018;5:68. doi: 10.3389/fcvm.2018.00068
37. Tohyama S, Hattori F, Sano M, Hishiki T, Nagahata Y, Matsuura T, Hashimoto H, Suzuki T, Yamashita H, Satoh Y, et al. Distinct metabolic flow enables large-scale purification of mouse and human pluripotent stem cell-derived cardiomyocytes. *Cell Stem Cell*. 2013;12:127–137. doi: 10.1016/j.stem.2012.09.013
38. Liang J, Wan M, Zhang Y, Gu P, Xin H, Jung SY, Qin J, Wong J, Cooney AJ, Liu D, et al. Nanog and Oct4 associate with unique transcriptional repression complexes in embryonic stem cells. *Nat Cell Biol*. 2008;10:731–739. doi: 10.1038/ncb1736
39. Baltus GA, Kowalski MP, Tutter AV, Kadam S. A positive regulatory role for the mSin3A-HDAC complex in pluripotency through Nanog and Sox2. *J Biol Chem*. 2009;284:6998–7006. doi: 10.1074/jbc.M807670200
40. Hoxha E, Lambers E, Wasserstrom JA, Mackie A, Ramirez V, Abramova T, Verma SK, Krishnamurthy P, Kishore R. Elucidation of a novel pathway through which HDAC1 controls cardiomyocyte differentiation through expression of SOX-17 and BMP2. *PLoS One*. 2012;7:e45046. doi: 10.1371/journal.pone.0045046
41. Wang Z, Zang C, Cui K, Schones DE, Barski A, Peng W, Zhao K. Genome-wide mapping of HATs and HDACs reveals distinct functions in active and inactive genes. *Cell*. 2009;138:1019–1031. doi: 10.1016/j.cell.2009.06.049
42. Kelly RD, Cowley SM. The physiological roles of histone deacetylase (HDAC) 1 and 2: complex co-stars with multiple leading parts. *Biochem Soc Trans*. 2013;41:741–749. doi: 10.1042/BST20130010
43. Huo JL, Jiao L, An Q, Chen X, Qi Y, Wei B, Zheng Y, Shi X, Gao E, Liu HM, et al. Myofibroblast deficiency of LSD1 alleviates TAC-induced heart failure. *Circ Res*. 2021;129:400–413. doi: 10.1161/CIRCRESAHA.120.318149
44. Gomez-Del Arco P, Perdiguero E, Yunes-Leites PS, Acin-Perez R, Zeini M, Garcia-Gomez A, Sreenivasan K, Jimenez-Alcazar M, Segales J, Lopez-Maderuelo D, et al. The chromatin remodeling complex Chd4/NuRD controls striated muscle identity and metabolic homeostasis. *Cell Metab*. 2016;23:881–892. doi: 10.1016/j.cmet.2016.04.008
45. Andersson C, Lin H, Liu C, Levy D, Mitchell GF, Larson MG, Vasan RS. Integrated multiomics approach to identify genetic underpinnings of heart failure and its echocardiographic precursors: Framingham heart study. *Circ Genom Precis Med*. 2019;12:e002489. doi: 10.1161/CIRCGEN.118.002489
46. Rivera C, Lee HG, Lappala A, Wang DN, Noches V, Olivares-Costa M, Sjöberg-Herrera M, Lee JT, Andrés ME. Unveiling RCOR1 as a rheostat at transcriptionally permissive chromatin. *Nat Commun*. 2022;13:1550. doi: 10.1038/s41467-022-29261-0